ELSEVIER Resources, Conservation and Recycling 25 (1999) 171–193

resources, conservation and recycling

A kinetic study of dye sorption by biosorbent waste product pith

Y.S. Ho, G. McKay *

Department of Chemical Engineering, The Hong Kong University of Science and Technology, Clear Water Bay, Kowloon, Hong Kong

Received 5 August 1998; accepted 12 August 1998

Abstract

The sorption of two dyes, namely, Basic Red 22 and Acid Red 114 onto pith has been studied in terms of pseudo-second-order, pseudo-first-order sorption and intraparticle diffusion processes thus comparing chemical sorption and diffusion sorption processes. The pseudo-second-order model, based on the assumption of a pseudo-second-order mechanism, has been developed to predict the rate constant of sorption, the equilibrium capacity and initial sorption rate as a function of the effect of initial dye concentration, pith particle size, pith dose and temperature.

Keywords: Pith; Dye; Kinetics; Sorption

1. Introduction

Environmental legislation has imposed stringent limits on the concentrations of pollutants which may be discharged in aqueous effluents. Consequently most industrial effluents require some form of treatment.

In recognition of the need for more complete treatment of wastewaters, an Advanced Waste Treatment Research (AWTR) programme was initiated in the

* Corresponding author. Tel.: +852 23587130; fax: +852 23580054.

0921-3449/99/$ - see front matter
PII S0921-3449(98)00053-6

USA during 1960. The objectives of this programme were to evaluate and develop additional and alternative treatment methods to produce a satisfactory effluent for discharge into receiving waters or for direct subsequent re-use as a water supply [1]. Various methods of wastewater treatment were examined within the AWTR programme and one of the most promising techniques to emerge for the removal of perdurable dissolved organic contaminants is adsorption [2].

The most widely used adsorbent for industrial applications is activated carbon. However, it is an expensive material unless regeneration is relatively easy, but this adds to the operational costs. Various cheap adsorbents have been tested [3] and give encouraging results in several areas of application. Activated silica has proved useful in treating textile mill effluent [4] and also for the adsorption of basic dyes [5,6]. Activated alumina has been used for the removal of phosphates from wastewaters [7]. Carbonaceous materials such as peat [8–11], wood [12,13] and lignite [14] have been used for the treatment of colour and metal ions in effluents. Other materials include fly ash [15] and rice husk, tree bark and human hair [16].

The present paper uses pith, a 'waste'/by-product from the sugar cane industry. In order to design adsorption treatment systems a knowledge of the kinetic and mass transfer processes is desirable. Therefore in the present paper three kinetic/mass transfer models are described and tested. These are a pseudo-first-order, a pseudo-second-order and an intraparticle diffusion model.

This present work applies the batch sorption results of two dyes, namely, Basic Red 22 (BB22) and Acid Red 114 (AR114) onto pith, to investigate the influence of intraparticle diffusion and a pseudo-second-order mechanism. It compares the rate parameter, k_i, of intraparticle diffusion, the rate parameter, k_2, of the pseudo-second-order and k_1, the rate parameter for the pseudo-first-order mechanisms.

2. Materials and methods

The adsorbent used in the study is bagasse pith, a waste product from the sugar cane industry. The Egyptian bagasse pith composition based on a chemical analysis is shown in Table 1. It was sieved into discrete particle size ranges.

Table 1
Chemical analysis of the bagasse pith

Determination	%
α-Cellulose	53.7
Pentosan	27.9
Lignin	20.2
Alcohol/benzene solubility	7.5
Ash	6.6

2.1. Sorbates

The sorbates and their structures used in the experiments are listed below. The dyestuffs were used as the commercial salts.

AR114 (Erionyl Red RS) CI 23635 was supplied by Ciba-Geigy.

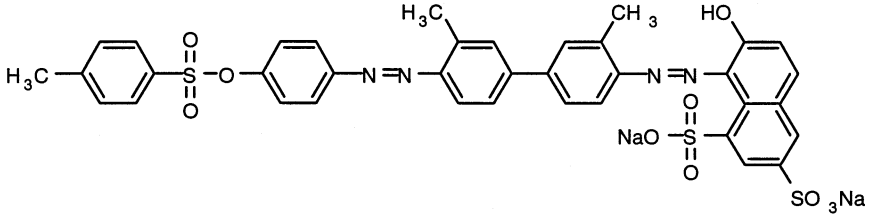

BR22 (Maxilon Red BL-N) CI 11055 was supplied by Ciba-Geigy.

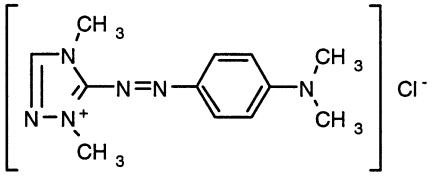

2.2. Method

The experimental results and methods are reported in a previous paper ([17]).

3. Results and discussion

3.1. Sorption dynamics

Sorption of dyes on pith may involve a chemical sorption which may control the reaction rate. In order to investigate the mechanism of sorption, the constants of sorption, and intraparticle diffusion of dyes were determined using equations of Lagergren [18], Weber and Morris [19] and a pseudo-second-order equation, respectively, which are as follows:

For a rate constant of first-order sorption

$$\log (q_1 - q_t) = \log(q_1) - \frac{k_1}{2.303} t \tag{1}$$

where q_1 is the amount of dyes sorbed at equilibrium (mg/g), q_t is the amount of dyes sorbed at time t (mg/g), k_1 is the equilibrium rate constant of first-order sorption (l/min).

Table 2
Parameters for effect of pith dose for BR22

m_s (g/dm^3)	r_2^2	q_2 (mg/g)	k_2 ($\times 10^4$ g/mg per min)	h (mg/g per min)	r_1^2	q_1 (mg/g)	k_1 ($\times 10^{-2}$ l/min)	r_i^2	k_i (mg/g per min$^{0.5}$)
0.25	0.989	78.8	4.45	2.76	0.986	60.9	1.12	0.980	4.78
0.5	0.997	74.4	4.35	2.41	0.980	57.2	1.04	0.971	4.66
0.75	0.991	72.0	4.23	2.19	0.987	57.1	1.04	0.981	4.48
1	0.992	69.7	4.04	1.96	0.993	56.3	1.00	0.985	4.37
1.25	0.991	66.0	4.23[4]	1.84	0.994	53.6	1.00	0.991	4.14
1.5	0.989	62.4	4.48	1.74	0.994	50.9	1.01	0.991	3.90

Table 3
Parameters for effect of pith dose for AR114

m_s (g/dm^3)	r_2^2	q_2 (mg/g)	k_2 ($\times 10^{-3}$ g/mg per min)	h (mg/g per min)	r_1^2	q_1 (mg/g)	k_1 ($\times 10^{-3}$ l/min)	r_i^2	k_i (mg/g per min$^{0.5}$)
0.50	0.979	15.4	1.53	0.363	0.991	13.2	9.55	0.993	0.964
0.75	0.978	14.9	1.51	0.336	0.996	12.8	9.28	0.997	0.933
1.00	0.970	14.5	1.48	0.313	0.995	12.7	9.22	0.998	0.907
1.25	0.970	14.6	1.45	0.308	0.994	12.7	9.08	0.996	0.913
1.50	0.976	13.9	1.59	0.306	0.996	12.0	9.20	0.997	0.870
2.00	0.980	13.2	1.54	0.283	0.996	11.8	8.96	0.997	0.847

The intercept of the straight line plots of $\log(q_1 - q_t)$ against t should be equal to $\log(q_1)$. If this is not the case, it suggests the reaction would not be a first-order reaction even if the linearized plots have higher correlation coefficients than the other two mechanisms.

In order to obtain the rate constants the straight line plots of $\log(q_t)$ against t for different dyes and difference conditions have been tested. The k_1 and correlation coefficients, r_1^2, values of dyes under different experimental conditions were calculated from these plots and are given in Tables 2 and 3.

The rate constant for pseudo-second-order sorption may be obtained from the following analysis:

$$\frac{dq_t}{dt} = k_2(q_2 - q_t)^2 \tag{2}$$

Separating the variables in Eq. (2) gives:

$$\frac{dq_t}{(q_2 - q_t)^2} = k_2\, dt \tag{3}$$

Integrating Eq. (3) for the boundary conditions $t = 0$ to $t = t$ and $q_t = 0$ to $q_t = q_t$, gives:

$$\frac{1}{(q_2 - q_t)} = \frac{1}{q_2} + k_2 t \tag{4}$$

which is the integrated rate law for a pseudo-second-order reaction, where q_2 is the amount of dyes sorbed at equilibrium (mg/g), k_2 is the equilibrium rate constant of pseudo-second-order sorption (g/mg per min). Eq. (4) can be rearranged to obtain a linear form:

$$\frac{t}{q_t} = \frac{1}{k_2 q_2^2} + \frac{1}{q_2} t \tag{5}$$

and

$$h = k_2 q_2^2 \tag{6}$$

where h is the initial sorption rate (mg/g per min).

The straight line plots of t/q_t against t have also been tested to obtain rate parameters. The k_2, q_2 and correlation coefficients, r_2^2, values of dyes under different conditions were calculated from these plots and are given in Tables 2 and 3.

The rate parameter of intraparticle diffusion can be defined as:

$$q = k_i t^{0.5} \tag{7}$$

where k_i is intraparticle diffusion rate constant (mg/g per $\text{min}^{0.5}$).

The k_i values under different conditions were calculated from the slopes of the straight line portions of the respective plots and are given in Tables 2 and 3.

3.2. Effect of pith dose

The effect of pith does was studied on the two dyes. Fig. 1 shows a series of contact time curves with pith dose varying from 0.25 to 1.5 g/dm^3. The results are also shown in Fig. 2 as a plot of t/q_t against t for sorption of BR22 for the pseudo-second-order model and in Fig. 3 as a plot of q_t against the square root of t for the intraparticle diffusion rate model for AR114 onto pith. The correlation coefficients, r_1^2, the first-order rate parameters, k_1, and sorption capacity, q_2, are shown in Tables 2 and 3 and compared with r_2^2, the pseudo-second-order rate parameters, k_2, and sorption capacity, q_2. The values of r_2^2 and r_1^2 are all extremely high (> 0.970). Although, based on the high correlation coefficients, it is difficult to distinguish between all three models, for the sorption of BR22 the results can be well represented by both the first-order and second-order model. However the equilibrium sorption capacity for second-order are slightly more reasonable than those of the first-order when comparing predicted results with experimental data because all of the equilibrium sorption capacities, q_1, are lower than experimental results.

In the case of AR114 sorption onto pith the correlation coefficients are the highest for the intrapaticle diffusion rate parameter suggesting the diffusion controlled mechanism is predominant. Therefore for AR114 sorption the r_2^2, r_1^2 values and the intraparticle diffusion coefficients are all high (> 0.97) with most of the r_i^2 values being slightly higher. This suggests that for acid dye sorption onto pith the

mechanism is predominantly intraparticle diffusion but the distinction is not completely clear. The overall rate of the basic dye sorption process appears to be controlled by the chemical process in this case in accordance with the pseudo-second-order reaction mechanism. Since the lignin component of the pith contains acid exchange groups due to fulvic and humic acids it seem likely that these could exchange with the ionic basic dye ions thus leading to the chemical sorption mechanism predominating for the basic dye system. Without the capability for ion exchange reactions the uptake capacity of acid dye is much less and the mechanism

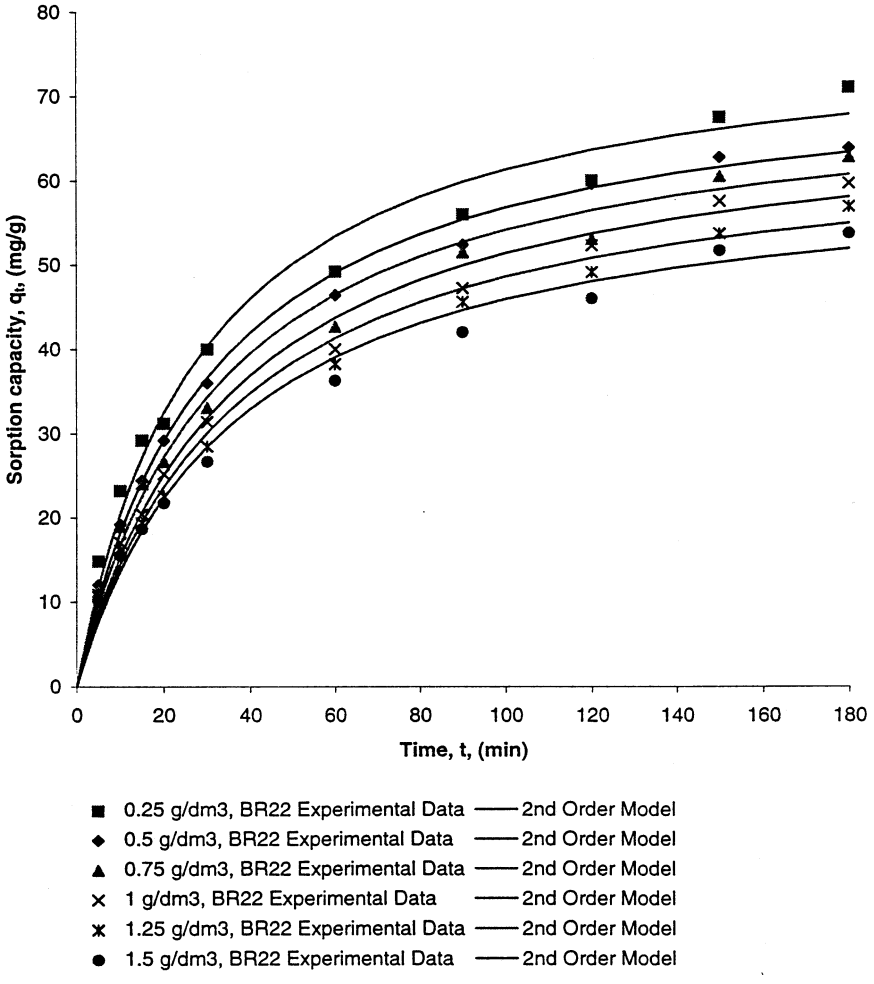

Fig. 1. Effect of pith dose on the sorption of BR22 onto pith. (■) 0.25 g/dm^3, BR22 experimental data—2nd order model; (◆) 0.5 g/dm^3, BR22 experimental data—2nd order model; (▲) 0.75 g/dm^3, BR22 experimental data—2nd order model; (X) 1.0 g/dm^3, BR22 experimental data—2nd order model; (ж) 1.25 g/dm^3, BR22 experimental data—2nd order model; (●) 1.25 g/dm^3, BR22 experimental data—2nd order model.

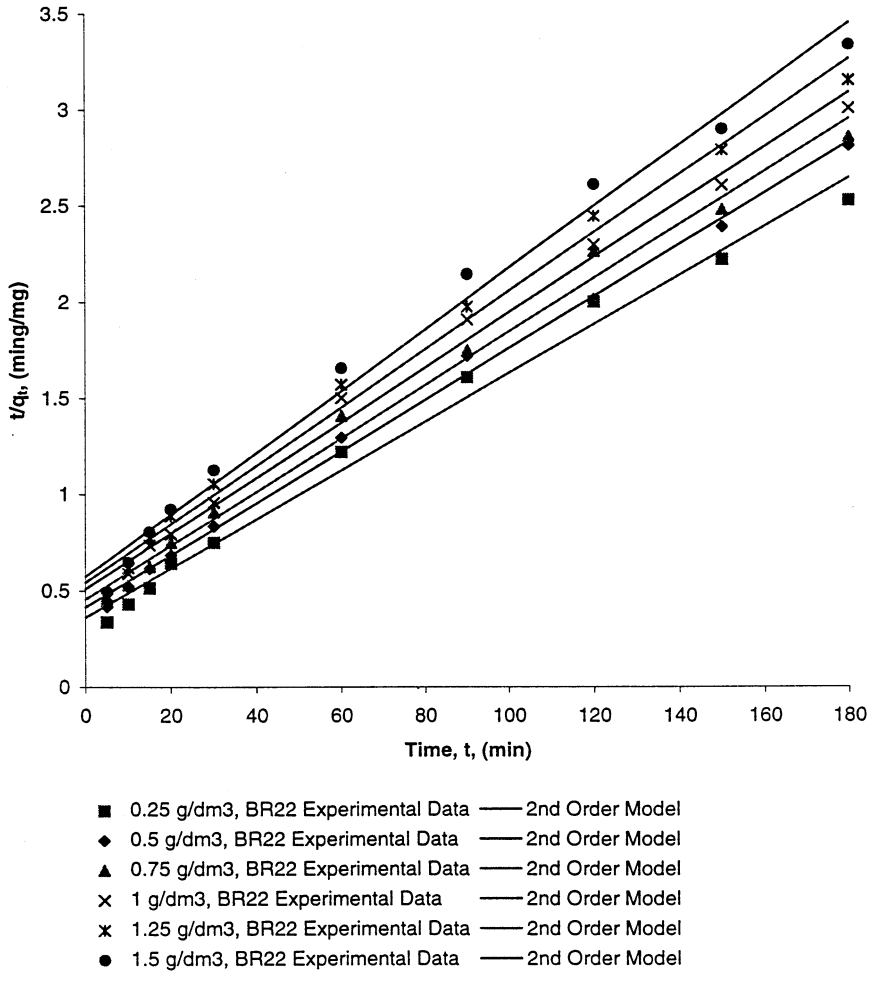

Fig. 2. Pseudo-second-order sorption kinetics of AR114 onto pith at various pith doses. (■) 0.25 g/dm^3, AR114 experimental data—2nd order model; (◆) 0.5 g/dm^3, AR114 experimental data—2nd order model; (▲) 0.75 g/dm^3, AR114 experimental data—2nd order model; (X) 1.0 g/dm^3, AR114 experimental data—2nd order model; (ж) 1.25 g/dm^3, AR114 experimental data—2nd order model; (●) 1.25 g/dm^3, AR114 experimental data—2nd order model.

is possibly physical diffusion which is well represented by the intraparticle diffusion $t^{0.5}$ plots.

The results in Tables 2 and 3 also show the sorption rate constant, k_2, initial sorption rate, h, and the equilibrium sorption capacity, q_2, as a function of pith dose. The pseudo-second-order rate constants, k_2, for the AR114 on the pith system show a decrease with pith dose from 0.5 to 1.25 g/dm^3 whereas the k_2 values for BR22 on pith are decreased with pith dose from 0.25 to 1 g/dm^3 and then increased with pith dose from 1 to 1.5 g/dm^3. The initial sorption rate, h, decreases with an

increase in the pith dose. Tables 2 and 3 show that h varies from 2.41 to 1.74 mg/g per min for BR22; and h varies from 0.363 to 0.306 mg/g per min for AR114 respectively for a pith dose variation from 0.5 to 1.5 g/dm^3. When increasing the pith dose from 0.5 to 1.5 g/dm^3 with an initial BR22 concentration of 200 mg/dm^3, the specific sorption at equilibrium, q_2, decreased from 74.4 to 62.4 mg/g and q_1 decreased from 57.2 to 50.9 mg/g for BR22 and from 0.5 to 1.5 g/dm^3 with an initial AR114 concentration of 100 mg/dm^3, the specific sorption at equilibrium, q_2, slightly decreased from 15.4 to 13.9 mg/g AR114 and q_1 slightly decreased from 13.2 to 12.0 mg/g AR114.

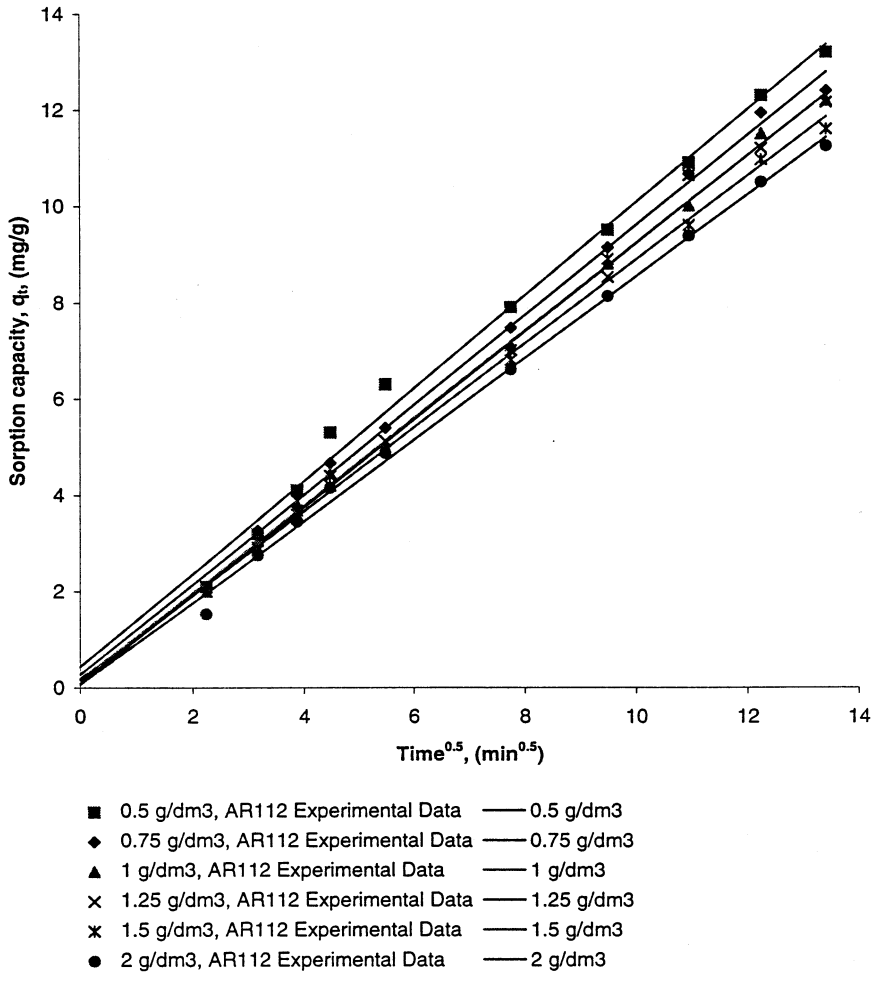

Fig. 3. Intraparticle diffusion kinetics of AR114 onto pith at various pith doses. (■) 0.5 g/dm^3, AR114 experimental data—0.5 g/dm^3; (◆) 0.75 g/dm^3, AR114 experimental data—0.75 g/dm^3; (▲) 1.0 g/dm^3, AR114 experimental data—1.0 g/dm^3; (X) 1.25 g/dm^3, AR114 experimental data—1.25 g/dm^3; (ж) 1.5 g/dm^3, AR114 experimental data—1.5 g/dm^3; (●) 2.0 g/dm^3, AR114 experimental data—2.0 g /dm^3.

Table 4
Empirical parameters for predicted q_2, k_2 and h from m_s

	A_q ($\times 10^{-2}$ g/mg)	B_q ($\times 10^{-3}$ g^2/mg per dm^3)	r^2	A_k (mg/min per g)	B_k (mg/min per dm^3)	r^2	A_h (g/ min per mg)	B_h (g^2/mg per dm^3)	r^2
BR22	1.66	−1.55	0.995	2.29×10^3	37.8	0.993	0.620	-9.48×10^{-2}	0.994
AR114	7.69	−7.56	0.998	6.38×10^2	23.4	0.994	3.76	−0.578	0.998

The corresponding linear plots of the values of q_2, k_2 and h against pith dose, m_s, were regressed to obtain expressions for these values in terms of the pith dose with high correlation coefficients (Table 4). Therefore it is further considered that q_2, k_2 and h can be expressed as a function of m_s for BR22 and AR114 as follows:

$$q_e = \frac{m_s}{A_q m_s + B_q} \tag{8}$$

$$k = \frac{m_s}{A_k m_s + B_k} \tag{9}$$

$$h = \frac{m_s}{A_h m_s + B_h} \tag{10}$$

Substituting the values of q_2 and h from Table 4 into Eqs. (8) and (10) and then into Eqs. (5) and (6), the rate law for a pseudo-second-order and the relationship of q_t, m_s and t can be represented as follows:

for BR22:

$$q_t = \frac{m_s t}{0.620 m_s - 9.48\times10^{-2} + (1.66\times10^{-2} m_s - 1.55\times10^{-3})t} \tag{11}$$

for AR114:

$$q_t = \frac{m_s t}{3.76 m_s - 0.578 + (7.69\times10^{-2} m_s - 7.56\times10^{-3})t} \tag{12}$$

Eqs. (11) and (12) represent generalised predictive models for the BR22 and AR114 sorbed at any contact time and pith dose within the given range. It indicated that the dye sorbed at any contact time is lower for a greater pith dose. These equations can then be used to derive the amount of dye sorbed at any given pith dose and the reaction time. The three dimensional plot of Eq. (11) is shown in Fig. 4 for BR114.

3.3. Effect of initial concentration

The experimental results of the sorption of BR22 on pith at various concentrations are shown in Fig. 5. The sorption capacity at equilibrium, q_2, increases from 40.7 to 82.8 mg/g with an increase in the concentration from 50 to 300 mg/dm^3 with

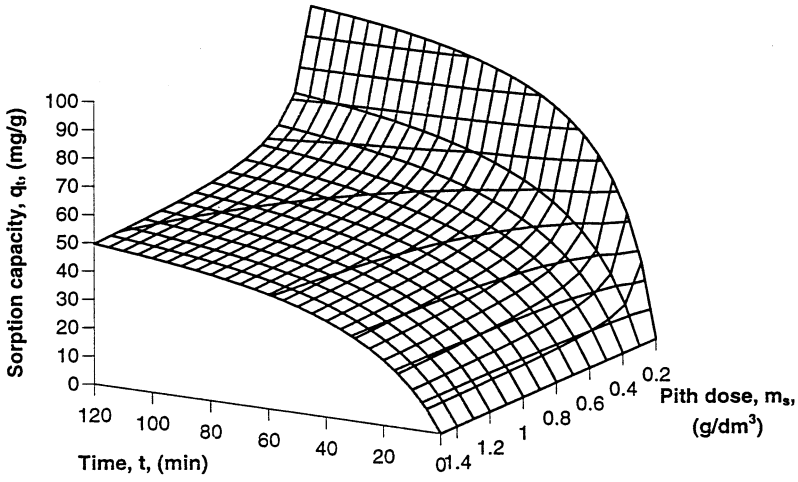

Fig. 4. Effect of pith dose on the sorption of BR22 onto pith at various reaction times.

Table 5
Parameters for effect of initial concentration for BR22

C_0 (mg/dm^3)	r_2^2	q_2 (mg/g)	k_2 ($\times 10^{-4}$ g/mg per min)	h (mg/g per min)	r_1^2	q_1 (mg/g)	k_1 ($\times 10^{-2}$ l/min)	r_i^2	k_i (mg/g per min)
50	0.988	40.7	7.44	1.23	0.993	32.6	1.05	0.989	2.52
100	0.987	53.4	5.50	1.57	0.998	43.2	1.03	0.994	3.30
150	0.986	65.1	4.73	2.00	0.998	52.1	1.06	0.995	4.00
200	0.990	73.5	4.35	2.35	0.996	57.8	1.06	0.988	4.52
250	0.989	77.3	4.50	2.69	0.989	60.1	1.12	0.979	4.68
300	0.994	82.8	4.23	2.90	0.993	63.2	1.09	0.979	5.06

Table 6
Parameters for effect of initial concentration for AR114

C_0 (mg/dm^3)	r_2^2	q_2 (mg/g)	k_2 ($\times 10^{-3}$ g/mg per min)	h (mg/g per min)	r_1^2	q_1 (mg/g)	k_1 (l/min)	r_i^2	k_i (mg/g per min$^{0.5}$)
25	0.997	5.63	7.36	0.233	0.968	4.72	1.87×10^{-2}	0.974	0.552
50	0.984	10.2	2.53	0.263	0.994	8.85	1.16×10^{-2}	0.995	0.753
75	0.973	14.6	1.18	0.253	0.997	13.2	8.21×10^{-3}	1.00	0.907
100	0.979	16.4	1.03	0.275	0.993	14.6	7.88×10^{-3}	0.993	1.01
125	0.982	16.3	1.31	0.349	0.994	14.2	9.09×10^{-3}	0.995	1.02
150	0.985	17.6	1.21	0.375	0.993	15.3	8.98×10^{-3}	0.995	1.11

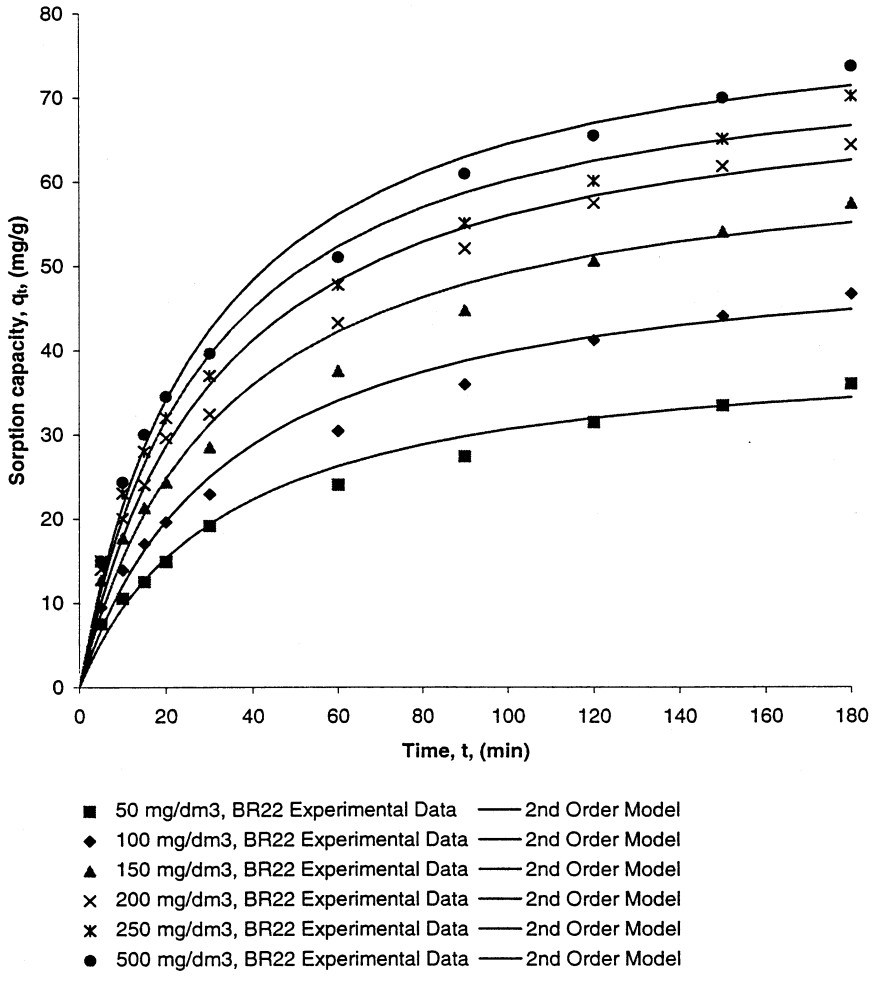

Fig. 5. Effect of initial concentration on the sorption of BR22 onto pith. (■) 50 mg/dm^3, BR22 experimental data—2nd order model; (◆) 100 mg/dm^3, BR22 experimental data—2nd order model; (▲) 150 mg/dm^3, BR22 experimental data—2nd order model; (X) 200 mg/dm^3, BR22 experimental data—2nd order model; (ж) 250 mg/dm^3, BR22 experimental data—2nd order model; (●) 500 mg/dm^3, BR22 experimental data—2nd order model.

a pith dose 1 g/dm^3 and an increase from 5.63 to 17.6 mg/g with an increase in the concentration from 25 to 150 mg/dm^3 with a pith dose 2 g/dm^3 for AR114. Fig. 6 shows a plot of t/q_t against t for the sorption of BR22 for the pseudo-second-order model and Fig. 7 shows a plot of q_t against the square root of t based on an intraparticle diffusion mechanism for AR114 onto pith. The correlation coefficients, r_1^2, the first-order rate parameters, k_1, and sorption capacity, q_1, are shown in Tables 5 and 6 and are compared with r_2^2, the pseudo-second-order rate parameters, k_2, and sorption capacity, q_2. For BR22 the values of r_2^2, r_1^2 and r_i^2 are all extremely

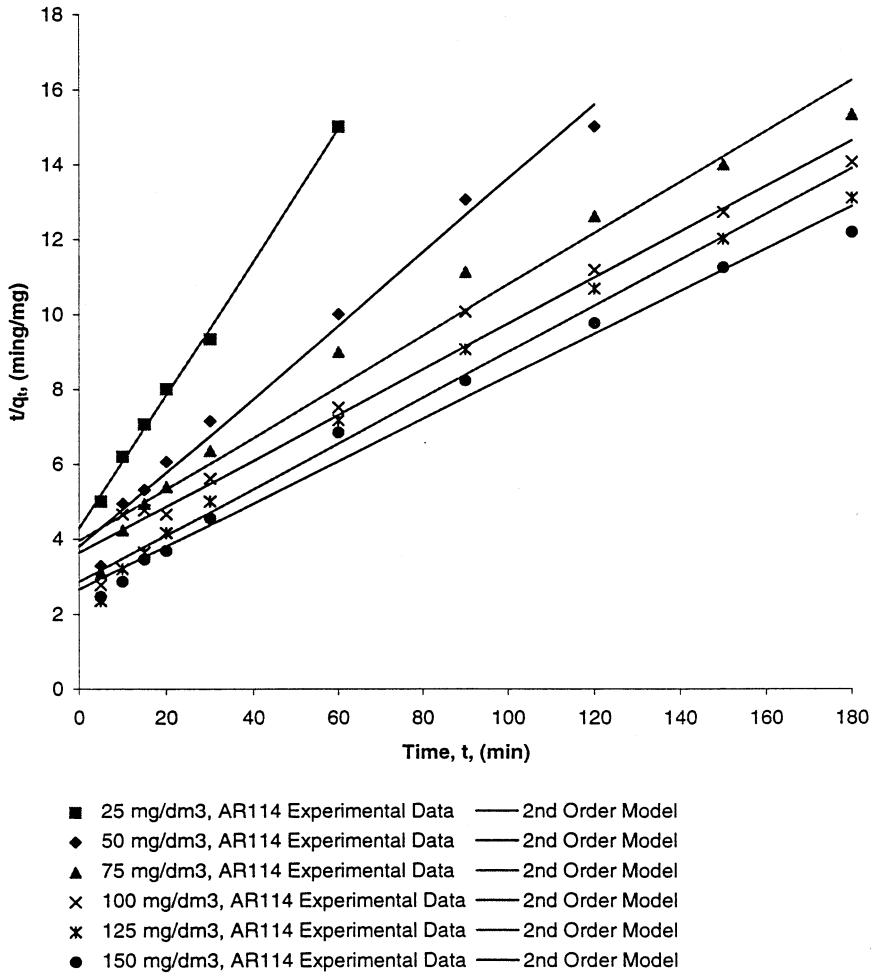

Fig. 6. Pseudo-second-order sorption kinetics of AR114 onto pith at various initial concentrations. (■) 25 mg/dm^3, AR114 experimental data—2nd order model; (◆) 50 mg/dm^3, AR114 experimental data—2nd order model; (▲) 75 mg/dm^3, AR114 experimental data—2nd order model; (X) 100 mg/dm^3, AR114 experimental data—2nd order model; (ж) 125 mg/dm^3, AR114 experimental data—2nd order model; (●) 150 mg/dm^3, AR114 experimental data—2nd order model.

Table 7
Empirical parameters for predicted q_2, k_2 and h from C_0

	A_q ($\times 10^{-2}$ g/mg)	B_q (g/dm^3)	r^2	A_k (mg/mim per g)	B_k (mg^2/min per g per dm^3)	r^2	A_h (g/min per mg)	B_h (g/min per dm^3)	r^2
BR22	9.41×10^{-3}	0.851	0.995	2.55×10^3	-6.53×10^4	0.998	0.235	35.7	0.960
AR114	3.38×10^{-2}	3.17	0.936	9.89×10^2	-1.93×10^4	0.947	2.33	82.4	0.903

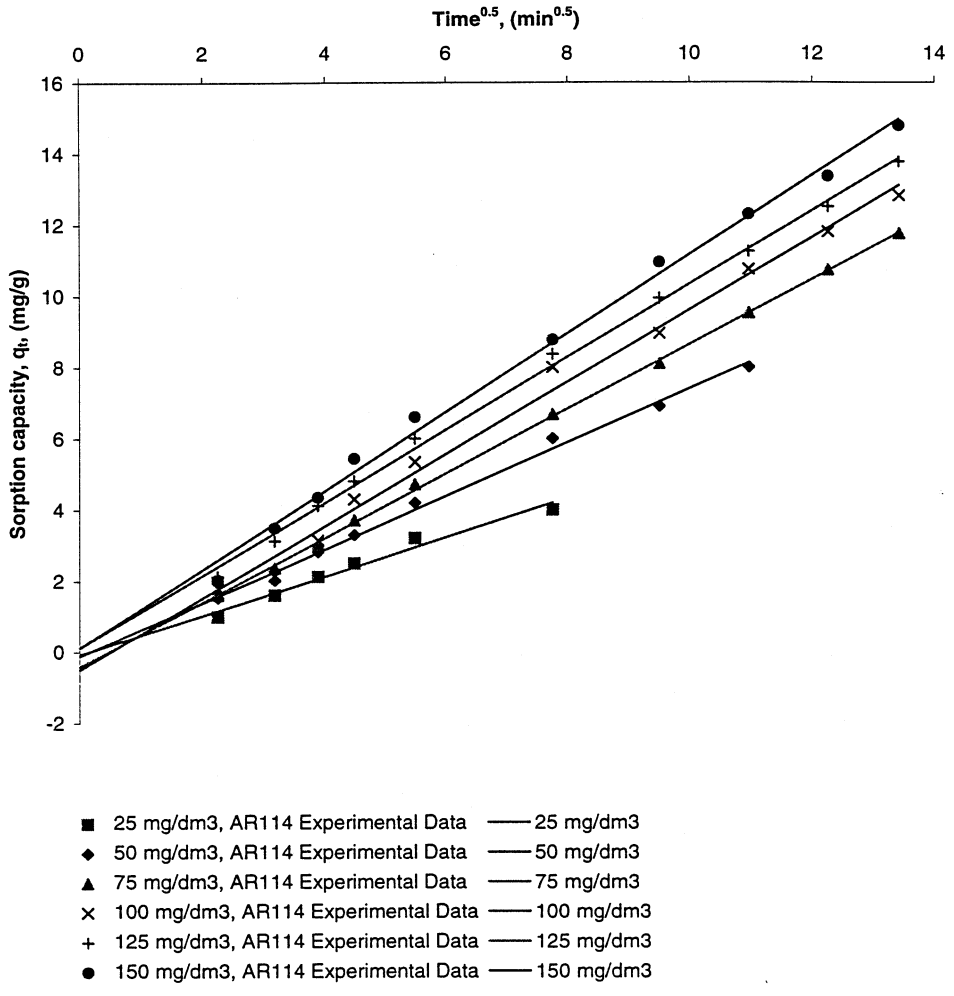

Fig. 7. Intraparticle diffusion kinetics of AR114 onto pith at various initial concentrations. (■) 25 mg/dm^3, AR114 experimental data—25 mg/dm^3; (◆) 50 mg/dm^3, AR114 experimental data—50 mg/dm^3; (▲) 75 mg/dm^3, AR114 experimental data—75 mg/dm^3; (X) 100 mg/dm^3, AR114 experimental data—100 mg/dm^3; (ж) 125 mg/dm^3, AR114 experimental data—125 mg/dm^3; (●) 150 mg/dm^3, AR114 experimental data—150 mg/dm^3.

high (>0.979). The optimum results are for both of the first-order and second-order models, with the first-order mechanism r_i^2 values being the highest. However, again the equilibrium sorption capacities for second-order correlation are much more reasonable when compared with experimental results than those of the first-order system. Since most of the first-order q_1 values deviate by almost 20% from the experimental values it suggests that the sorption of BR22 onto pith follows the pseudo-second-order model.

For the sorption of AR114 the r_2^2, r_1^2 and r_i^2 values are all high (>0.973) with all of the r_i^2 values being slightly higher. Figs. 7 and 8 show plots of the amount of AR114 and BR22 per unit weight of pith against the square root of t generates the best fit straight lines that pass close through the origin. This suggests that for dye sorption onto pith the mechanism is predominantly intraparticle diffusion particularly for AR114, although the overall rate of the sorption process for BR22 appears to be influenced by the chemical process in this case in accordance with the ionic exchange processes discussed previously.

The corresponding linear plots of the values of q_2, k_2 and h against initial dye concentration, C_0, were regressed to obtain expressions for these values in terms of the initial dye concentration with high correlation coefficients (Table 7). Therefore it is useful for process design purposes if q_2, k_2 and h can be expressed as a function of C_0 for BR22 and AR114 as follows:

$$q_e = \frac{C_0}{A_q C_0 + B_q} \tag{13}$$

$$k = \frac{C_0}{A_k C_0 + B_k} \tag{14}$$

$$h = \frac{C_0}{A_h C_0 + B_h} \tag{15}$$

Substituting the values of q_2 and h from Table 7 into Eqs. (13) and (15) and then into Eqs. (5) and (6), the rate law for a pseudo-second-order and the relationship of q_t, C_0 and t can be represented as follows:

for BR22:

$$q_t = \frac{C_0 t}{0.235 C_0 + 35.7 + (9.41 \times 10^{-3} C_0 + 0.851)t} \tag{16}$$

for AR114:

$$q_t = \frac{C_0 t}{2.33 C_0 + 82.4 + (338 \times 10^{-2} C_0 + 3.17)t} \tag{17}$$

Eqs. (16) and (17) represent generalised predictive models for the BR22 and AR114 sorbed at any contact time and initial concentration within the given ranges. It indicates that the dye sorbed at any contact time per unit mass is higher for a greater initial concentration. These equations can be used to derive the amount of dye sorbed at any given initial concentration and the reaction time.

3.4. Effect of particle size

The results of the effect of pith particle size on experiments carried out using the same initial dye concentration 200 mg/dm^3 with pith dose 1 g/dm^3 for BR22 and 100 mg/dm^3 with pith dose 2 g/dm^3 for AR114 are shown in Figs. 9 and 10. Results from a series of kinetics experiments at four pith particle size ranges from 150–250 to 710–1000 μm are shown in Tables 8 and 9. The data for BR22 again show a

good compliance with the pseudo-second-order equation and the regression coefficients, r_2^2, for the linear plots were all high (>0.993). It was found that the equilibrium sorption of dye, q_2, the rate constant, k_2, and the initial sorption rate, h, are a function of pith particle size. The initial sorption rate decreased with an increase in the pith particle size. While the initial sorption rate varied from 5.58 to 1.95 mg/g per min as the pith particle size was varied from 150–250 to 710–1000 μm for BR22 and from 0.943 to 0.359 mg/g per min for the case of AR114.

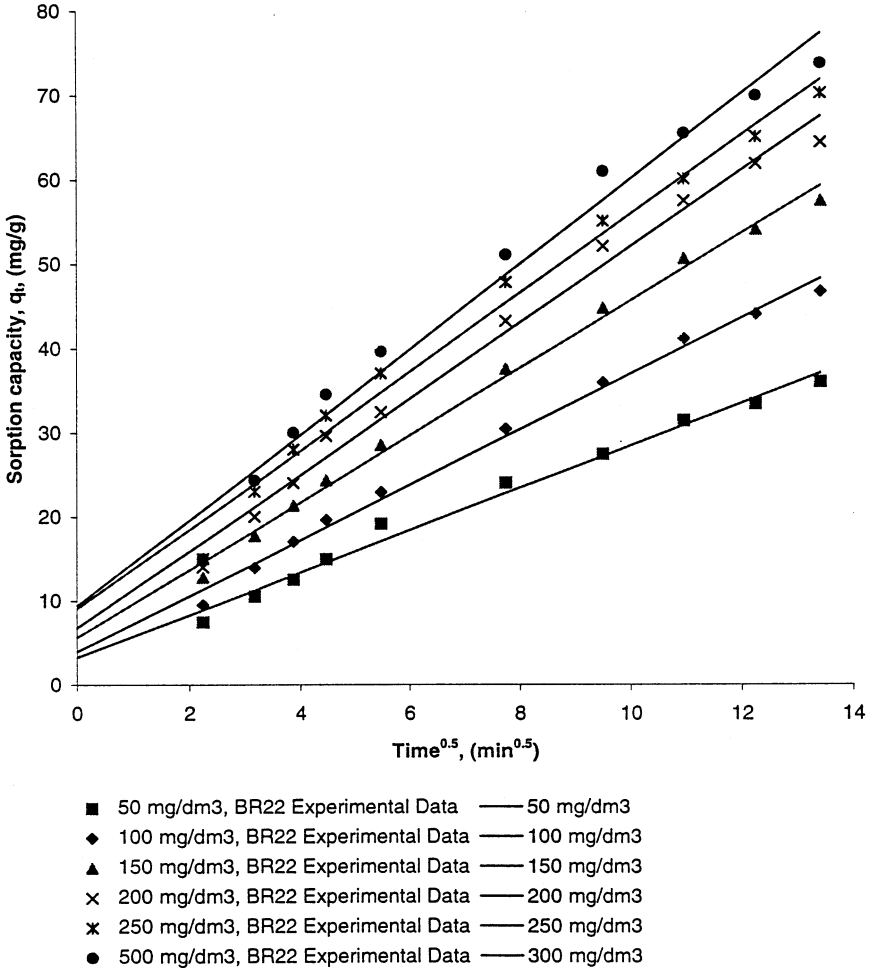

Fig. 8. Intraparticle diffusion kinetics of BR22 onto pith at various initial concentrations. (■) 50 mg/dm^3, BR22 experimental data—50 mg/dm^3; (◆) 100 mg/dm^3, BR22 experimental data—100 mg/dm^3; (▲) 150 mg/dm^3, BR22 experimental data—150 mg/dm^3; (X) 200 mg/dm^3, BR22 experimental data—200 mg/dm^3; (ж) 250 mg/dm^3, BR22 experimental data—250 mg/dm^3; (●) 500 mg/dm^3, BR22 experimental data—300 mg/dm^3.

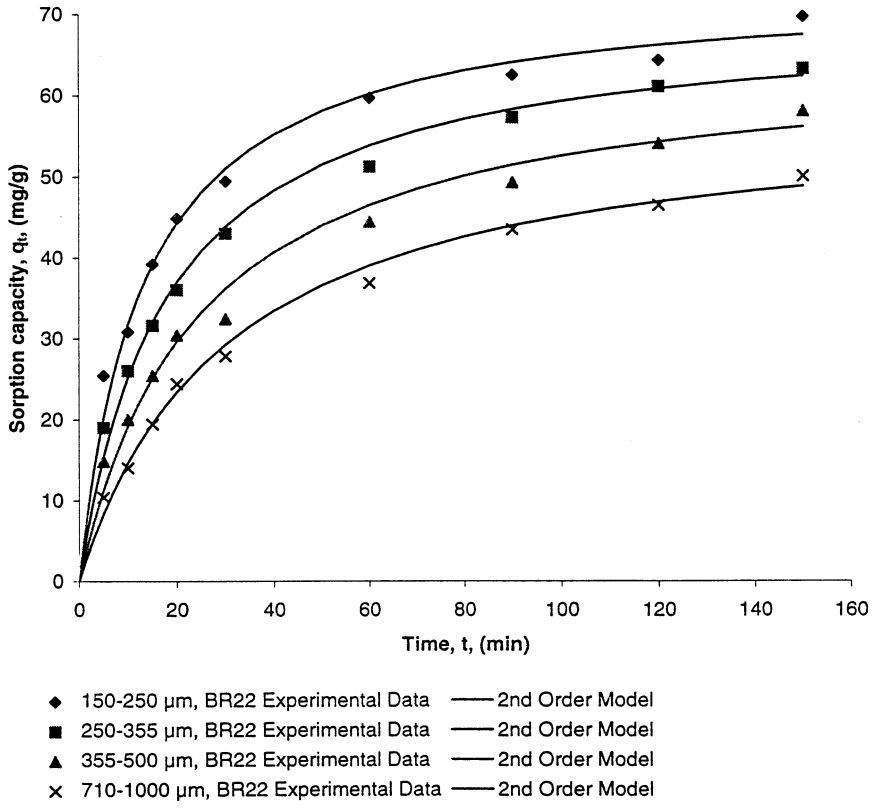

Fig. 9. Effect of pith particle size on the sorption of BR22 onto pith. (◆) 150–250 μm, BR22 experimental data—2nd order model; (■) 250–355 μm, BR22 experimental data—2nd order model; (▲) 355–500 μm, BR22 experimental data—2nd order model; (X) 710–1000 μm, BR22 experimental data—2nd order model.

Table 8
Parameters for effect of pith particle size for BR22

d_p (μm)	r_2^2	q_2 (mg/g)	k_2 (g/mg per min)	h (mg/g per min)	r_1^2	q_1 (mg/g)	k_1 ($\times 10^{-2}$ l/min)	r_i^2	k (mg/g per min$^{0.5}$)
150–250	0.997	73.3	1.04×10^{-3}	5.58	0.959	43.6	1.56×10^{-2}	0.925	4.15
250–355	0.998	69.6	8.13×10^{-4}	3.94	0.983	46.4	1.39	0.955	4.32
355–500	0.993	65.0	6.43×10^{-4}	2.72	0.992	48.8	1.28	0.979	4.23
710–1000	0.995	58.6	5.68×10^{-4}	1.95	0.987	46.3	1.16	0.977	3.96

The correlation coefficients, r_1^2, the first-order rate parameters, k_1, and sorption capacity, q_1, are shown in Tables 8 and 9 and compared with r_2^2, the pseudo-second-order rate parameters, k_2, and sorption capacity, q_2. The values of r_2^2 and r_1^2 are all

high (> 0.952) but in all cases the r_2^2 values are higher. In addition, all of the equilibrium sorption capacities, q_1, are much lower than experimental results. Again, it suggests that the sorption of BR22 and AR114 onto pith follows the pseudo-second-order model.

Table 9
Parameters for effect of pith particle size for AR114

d_p (μm)	r_2^2	q_2 (mg/g)	k_2 ($\times 10^{-3}$ g/mg per min)	h (mg/g per min)	r_i^2	q_1 (mg/g)	k_1 ($\times 10^{-2}$ l/min)	r_i^2	k (mg/g per min$^{0.5}$)
150-250	0.999	18.6	2.73	0.943	0.960	12.6	1.32	0.915	1.20
250–355	0.998	16.2	3.07	0.809	0.965	11.1	1.31	0.916	1.05
355–500	0.998	15.3	2.15	0.499	0.952	11.7	1.10	0.939	1.05
710–1000	0.995	12.3	2.38	0.359	0.976	9.88	1.08	0.964	8.40

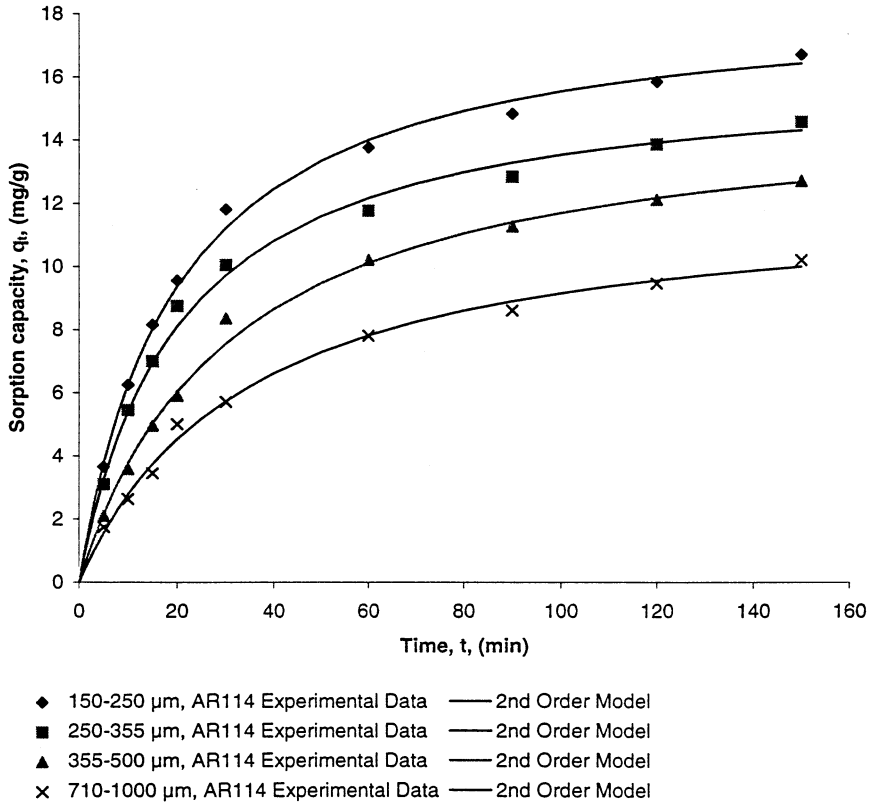

Fig. 10. Effect of pith particle size on the sorption of AR114 onto pith. (◆) 150–250 μm, AR114 experimental data—2nd order model; (■) 250–355 μm, AR114 experimental data—2nd order model; (▲) 355–500 μm, AR114 experimental data—2nd order model; (X) 710–1000 μm, AR114 experimental data—2nd order model.

Table 10
Parameters for effect of temperature for BR22

T (°C)	r_2^2	q_2 (mg/g)	k_2 ($\times 10^{-4}$ g/mg per min)	h (mg/g per min)	r_1^2	q_1 (mg/g)	k_1 (l/min)	r_i^2	k_i (mg/g per min$^{0.5}$)
20	0.994	74.2	2.75	1.52	0.992	65.1	9.28×10^{-3}	0.993	5.00
40	0.994	82.0	2.99	2.01	0.991	69.7	1.02×10^{-2}	0.990	5.60
60	0.997	90.5	3.62	2.97	0.978	71.3	1.14×10^{-2}	0.974	6.19
80	0.997	100	3.99	4.02	0.982	75.1	1.23×10^{-2}	0.967	6.70

Table 11
Parameters for effect of temperature for AR114

T (°C)	r_2^2	q_2 (mg/g)	k_2 ($\times 10^{-3}$ g/mg per min)	h (mg/g per min)	r_1^2	q_1 (mg/g)	k_1 ($\times 10^{-2}$ l/min)	r_i^2	k_i (mg/g per min$^{0.5}$)
20	0.997	12.5	2.89	0.453	0.971	9.61	1.19	0.960	0.849
40	0.993	15.1	2.34	0.536	0.984	11.8	1.19	0.970	1.01
60	0.998	16.2	2.69	0.702	0.974	11.7	1.26	0.953	1.07
80	0.999	18.7	2.50	0.871	0.961	13.1	1.29	0.937	1.23

3.5. Effect of temperature

The temperature dependence of sorption was studied with a constant initial dye concentration of 200 mg/dm^3 for BR22 and 100 mg/dm^3 for AR114, and pith dose 1 g/dm^3 for BR22 and 2 g/dm^3 for AR114 at with various temperatures of reaction sorption (Figs. 11 and 12). Figs. 13 and 14 show good compliance with the pseudo-second-order equation. The experimental points are shown together with the theoretically generated curves. The agreement between the sets of data reflect the extremely high correlation coefficients obtained and shown in Tables 10 and 11. The correlation coefficients, r_1^2, the first-order rate parameters, k_1, and sorption capacity, q_1, are shown in Tables 10 and 11 and compared with r_2^2, the pseudo-second-order rate parameters, k_2, and sorption capacity, q_2. The values of r_2^2 and r_1^2 are all extremely high (>0.961). The results can fit both the pseudo-first-order and the pseudo-second-order models. Again, the equilibrium sorption capacities for pseudo-second-order are much more reasonable than those predicted by the pseudo-first-order kinetics when compared with experimental results because all of the equilibrium sorption capacities, q_1, are lower than the experimental equilibrium results. Both dye/pith systems show extremely high reaction correlation coefficients, r_2^2, which are all greater than 0.993. The intraparticle coefficients, r_i^2, are lower than r_2^2. These results suggest that the sorption of BR22 and AR114 onto pith follow the pseudo-second-order model.

The initial sorption rate, h, increases with an increase in the temperature. Tables 10 and 11 show that h varies from 1.52 to 4.02 mg/g per min for BR22; and h varies from 0.453 to 0.871 mg/g per min for AR114, respectively, for a temperature variation from 20 to 80°C. On increasing the temperature from 20 to 80°C, the specific sorption at equilibrium, q_2, increased from 74.2 to 100 mg/g for BR22; and from 12.5 to 18.7 mg/g for AR114. The increase in the equilibrium sorption of dye with temperature indicates that a high temperature favors dye removal by adsorption on the pith. The sorption of dye by pith may involve not only physical but also chemical sorption. The values of the rate constant, k_2, were found to increase from 2.75×10^4 to 3.99×10^4 g/mg per min, for an increase in the solution temperature from 293 to 353 K for the sorption of BR22 and from 2.89×10^{-3} to 50×10^{-3} g/mg per min, for an increase in the solution temperature from 293 to 353 K for the sorption of AR114.

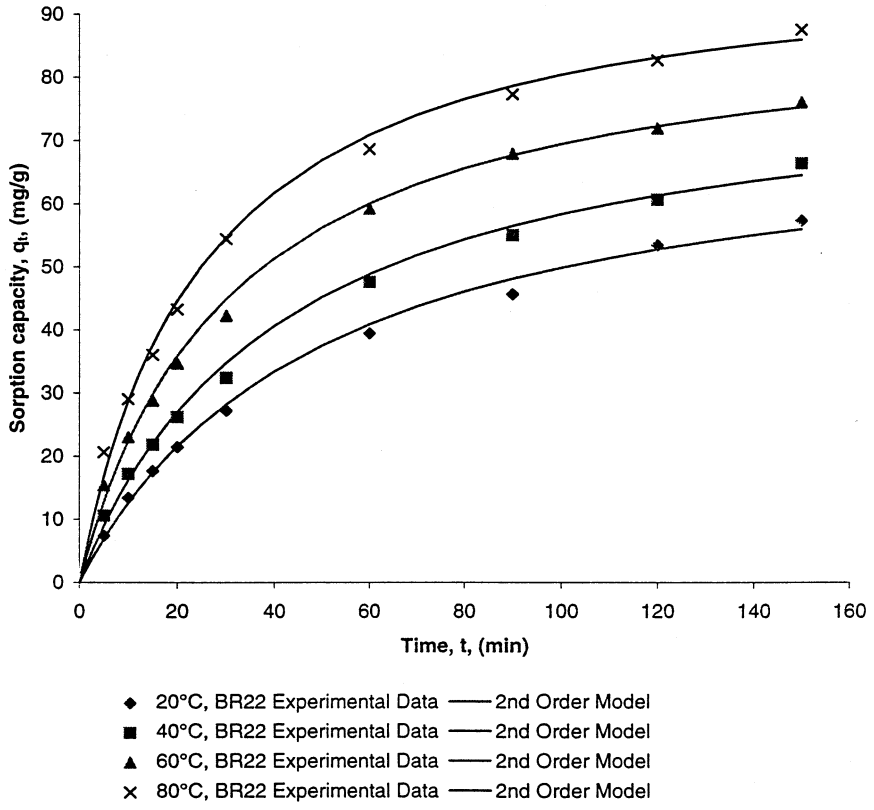

Fig. 11. Effect of temperature on the sorption of BR22 onto pith. (◆) 20°C, BR22 experimental data—2nd order model; (■) 40°C, BR22 experimental data—2nd order model; (▲) 60°, BR22 experimental data—2nd order model; (X) 80°C, BR22 experimental data—2nd order model.

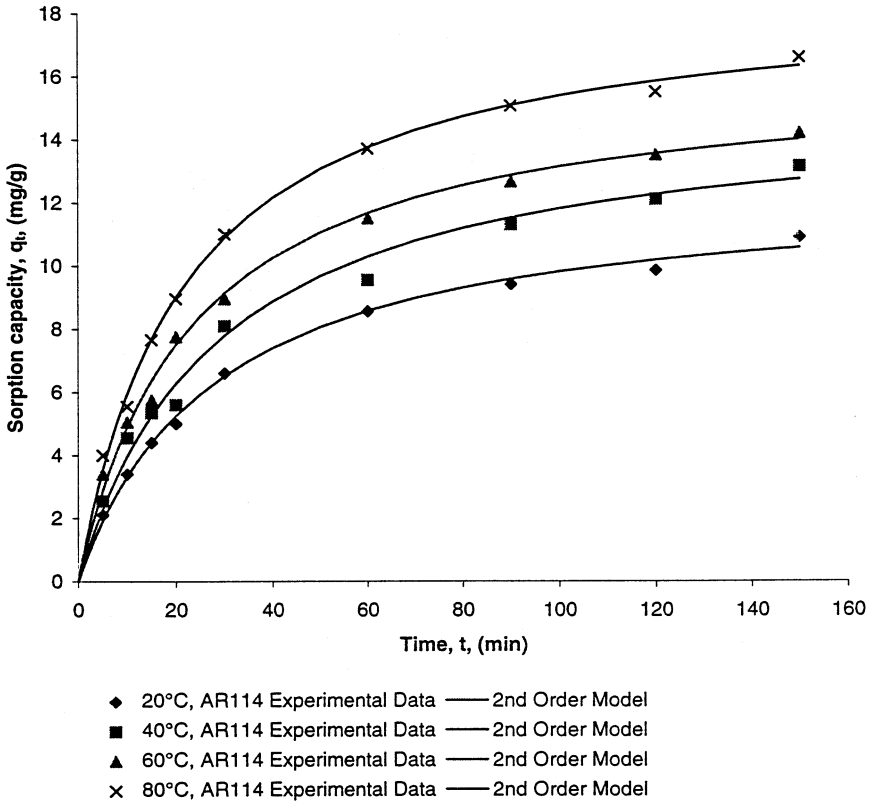

Fig. 12. Effect of temperature on the sorption of AR114 onto pith. (◆) 20°C, AR114 experimental data—2nd order model; (■) 40°C, AR114 experimental data—2nd order model; (▲) 60°, AR114 experimental data—2nd order model; (X) 80°C, AR114 experimental data—2nd order model.

The rate constant, k_2, for the second-order BR22 sorption reaction show an Arrhenius dependence on reciprocal absolute temperature. The same trend is observed for BR22 using the intraparticle diffusion rate parameter k_i and an activation energy for the sorption process of approximately 5 kJ/mol is obtained for both mechanisms. The magnitude of this value is quite low, particularly for a reaction type process and it is more consistent of a physical sorption process. In the case of AR114 the pseudo-second-order rate constants are relatively constant and indicate the sorption process is not activated. However, analysing the intraparticle diffusion rate parameters by the Arrhenius equation does yield an activation energy but it is less than 2 kJ/mol. Therefore the adsorption of AR114 onto pith does appear to be a low energy physisorption process.

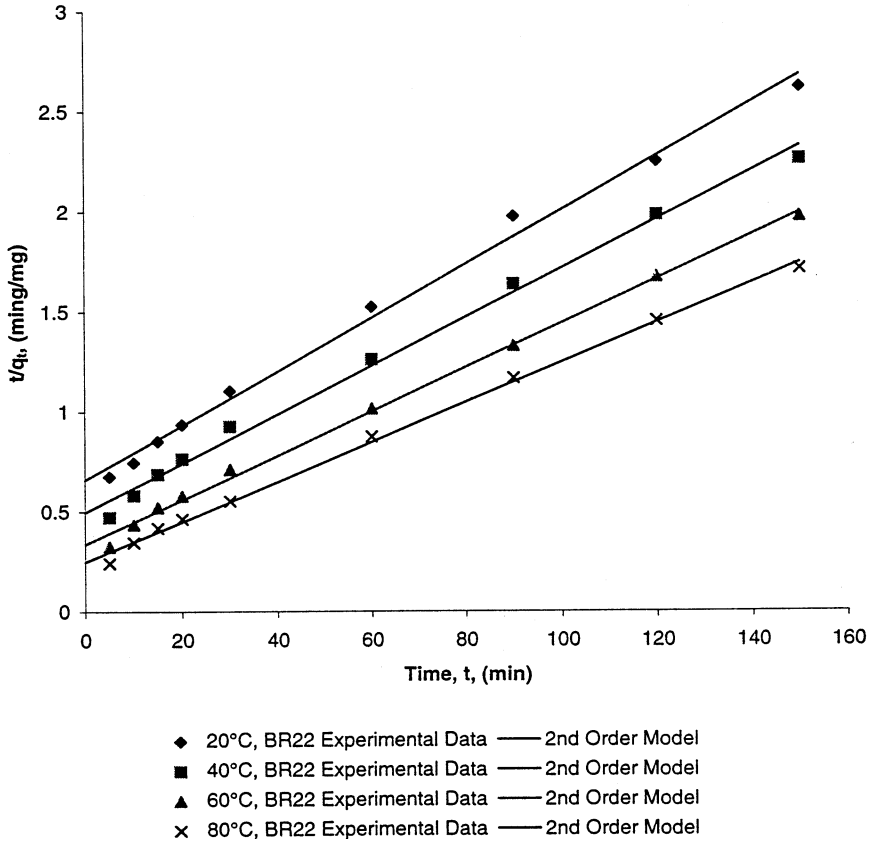

Fig. 13. Pseudo-second-order kinetic plot for the sorption of BR22 onto pith at various temperatures. (◆) 20°C, BR22 experimental data—2nd order model; (■) 40°C, BR22 experimental data—2nd order model; (▲) 60°, BR22 experimental data—2nd order model; (X) 80°C, BR22 experimental data—2nd order model.

4. Conclusion

The kinetics of sorption of BR22 and AR114 on pith were studied on the basis of the pseudo-second-order rate mechanism. The sorption of capacity of basic dye (BR22) is much higher than acid dye (AR114) because of the ionic charges on the dyes and the character of the pith. The sorption of BR22 and AR114 by pith are exothermic process activated processes. For both dye/pith systems, the pseudo-first-order chemical reaction does not provide the best fit models overall in the rate controlling step, the sorption of dyes onto pith is best described by the pseudo-second-order chemical reaction kinetics which provide the best correlation of the data in most cases. While the sorption of BR22 dye seems to follow a pseudo-second-order sorption reaction mechanism when the effects of initial dye concentration, adsorbent mass and solution temperature are investigated, the mechanism for

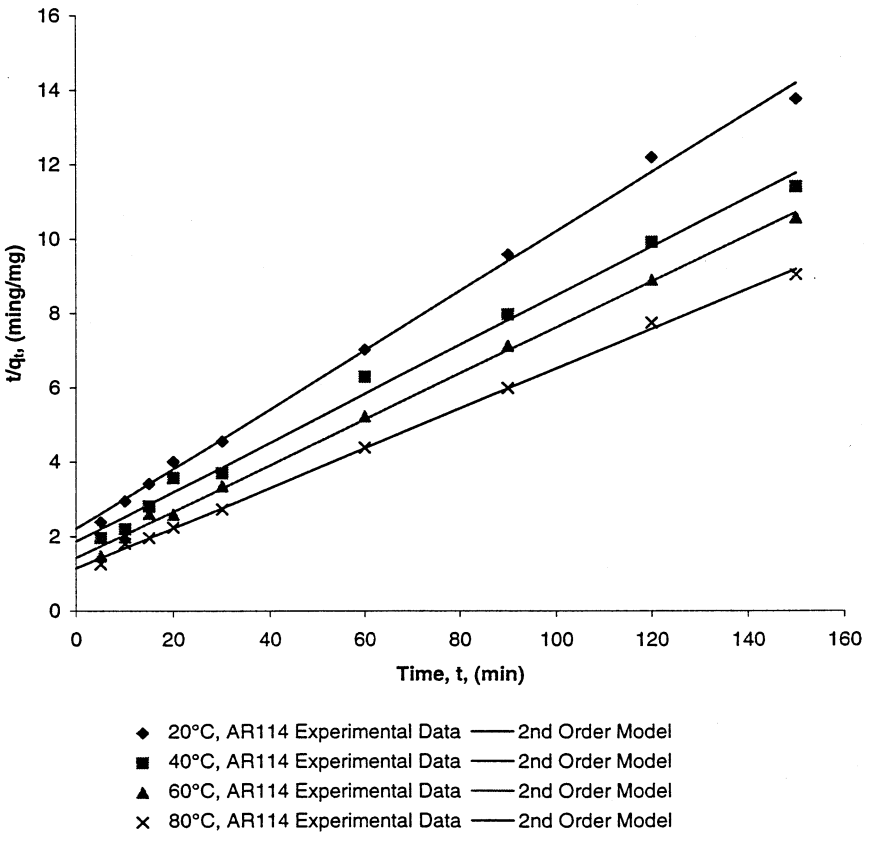

Fig. 14. Pseudo-second-order kinetic plot for the sorption of AR114 onto pith at various temperatures. (◆) 20°C, AR114 experimental data—2nd order model; (■) 40°C, AR114 experimental data—2nd order model; (▲) 60°, AR114 experimental data—2nd order model; (X) 80°C, AR114 experimental data—2nd order model.

AR114 is not as clearly apparent. The rate controlling step appears to be well correlated by both mechanisms to a certain extent and the extent of this control seems to have a dependence on the system conditions.

References

[1] Morris JC, Weber WJ, Jr. Preliminary appraisal of advanced waste treatment processes. Public Health Serv Publ 1962:W62–24.
[2] Weber WJ, Morris JC. Equilibrium and capacities for adsorption on carbon. J Sanit Eng Div Am Soc Civ Eng 1964;90:79–91.
[3] Williamson JN, Heit AH, Calmon C. Adsorbants for effluent treatment. Public Health Service Publications. 1964;No. 999-SP-14:12–23.
[4] Middleton AB. How acticated silica is used to treat water in textile mills. Am Dyestuffs Report 1971;August:26–29.

[5] Allingham MM, Cullen JM, Giles CH, Jain SK, Woods JS. Adsorption at inorganic surfaces. II. Adsorption of dyes and related compounds by silica. J Appl Polym Sci 1958;8:108–18.
[6] McKay G, Alexander F. Kinetics of the removal of basic dye from effluent using silica. Chem Eng 1977;319:243–6.
[7] Gangoli N. Phosphate removal by activated alumina. MSc Thesis, Northwestern University Evaston, 1971.
[8] Poots VJP, McKay G, Healy JJ. The removal of acid dye from effluent using natural adsorbents-I Peat. Water Res 1976;10:1061–6.
[9] McKay G, Allen SJ. Surface mass transfer processes using peat as an adsorbent for dyestuffs. Can J Chem Eng 1980;58:521–6.
[10] Gosset T, Trancart JL, Thevenot DR. Batch metal removal by peat kinetics and thermodynamics. Water Res 1986;20:21–6.
[11] Ho YS, Wase DAJ, Forster CF. The adsorption of divalent copper ions from aqueous solution by sphagnum moss peat. Trans I Chem Eng Part B 1994;17:185–94.
[12] Poots VJP, McKay G, Healy JJ. The removal of acid dye from effluent using natural adsorbents-II Wood. Water Res 1976;10:1067–1071.
[13] McKay G, McConvey IF. The external mass-transfer of basic and acidic dyes on wood. J Chem Technol Biotech 1981;31:401–8.
[14] Allen SJ, McKay G, Khader KYH. Equilibrium adsorption isotherms fro basic dyes on lignite. J Chem Technol Biotech 1989;45:291–302.
[15] Khare SK, Panday KK, Srivastava RM, Singh VN. Removal of Victoria Blue from aqueous solution by fly ash. J Chem Technol Biotech 1987;38:99–104.
[16] McKay G, El Geundi M, Nassar MM. Equilibrium studies during the removal of dyestuffs from aqueous solutions using bagasse pith. Water Res 1987;21:1513–20.
[17] McKay G, Ramprasad G, Mowli P. Desorption and regeneration of dye colors from low-cost materials. Water Res 1987;21:375–7.
[18] Lagergren S. Zur theorie der sogenannten adsorption geloster stoffe. Kungliga Svenska Vetenskapsakademiens. Handlingar, Band 24, 1898;4:1–39.
[19] Weber WJ, Morris JC. Intraparticle diffusion during the sorption of surfactants onto activated carbon. J Sanit Eng Div Am Soc Civ Eng 1963;89:53–61.